
Swing-Up and Stabilization of a Cart Pendulum System and Stabilization of a Twin Pendulum System

Using Nonlinear Control Strategies

Master Thesis

Aalborg University
Control & Automation
Fredrik Bajers Vej 7
DK-9220 Aalborg

by
Niels Skov Vestergaard



Master Thesis

Control and Automation

Department of Electronic Systems

Fredrik Bajers Vej 7C

9220 Aalborg

Synopsis:

Title:

Swing-Up and Stabilization of a Cart Pendulum System and Stabilization of a Twin Pendulum System

Subtitle:

Using Nonlinear Control Strategies

Theme:

Nonlinear Control

Project Period:

Autumn 2018

Participants:

Niels Skov Vestergaard

Supervisor:

John-Josef Leth

Pages: ?

Appendices: ?

Attachments: ?

Concluded: 2019-01-16

Nam dui ligula, fringilla a, euismod sodales, sollicitudin vel, wisi. Morbi auctor lorem non justo. Nam lacus libero, pretium at, lobortis vitae, ultricies et, tellus. Donec aliquet, tortor sed accumsan bibendum, erat ligula aliquet magna, vitae ornare odio metus a mi. Morbi ac orci et nisl hendrerit mollis. Suspendisse ut massa. Cras nec ante. Pellentesque a nulla. Cum sociis natoque penatibus et magnis dis parturient montes, nascetur ridiculus mus. Aliquam tincidunt urna. Nulla ullamcorper vestibulum turpis. Pellentesque cursus luctus mauris.

Nam dui ligula, fringilla a, euismod sodales, sollicitudin vel, wisi. Morbi auctor lorem non justo. Nam lacus libero, pretium at, lobortis vitae, ultricies et, tellus. Donec aliquet, tortor sed accumsan bibendum, erat ligula aliquet magna, vitae ornare odio metus a mi. Morbi ac orci et nisl hendrerit mollis. Suspendisse ut massa. Cras nec ante. Pellentesque a nulla. Cum sociis natoque penatibus et magnis dis parturient montes, nascetur ridiculus mus. Aliquam tincidunt urna. Nulla ullamcorper vestibulum turpis. Pellentesque cursus luctus mauris.

Publication of this report's contents (including citation) without permission from the authors is prohibited

Contents

1	Introduction	1
Part I Cart Pendulum		2
2	System and Model	3
2.1	System	3
2.2	Model	5
Part II Twin Pendulum		8
Appendix		9

1 | Introduction

Two parts - two different systems and control objectives.

Part I

Cart Pendulum

2 | System and Model

A brief overview of the relevant system for *Part 1* is presented in this chapter along with a model of the system.

2.1 System

A setup is provided by the Control and Automation Department at Aalborg University (AAU), see Figure 2.1.

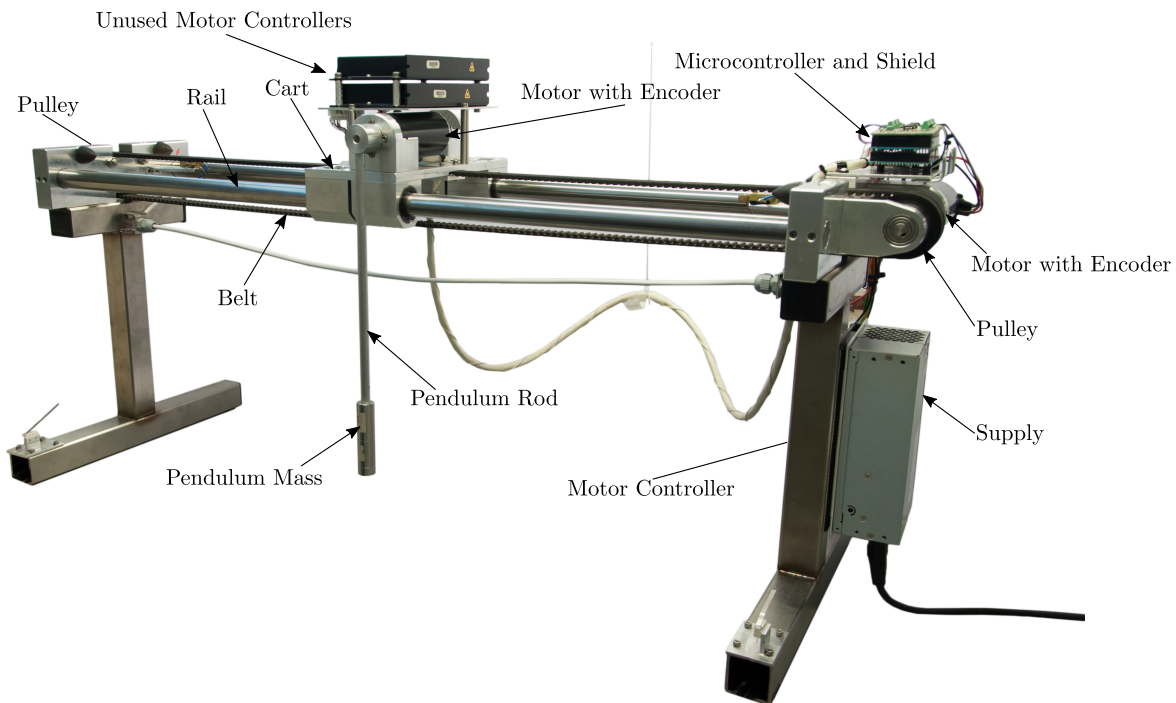


Figure 2.1: The setup provided by AAU. The motor controller in use is not directly visible in this picture as it is mounted behind the power supply.

As seen in Figure 2.1 the belt is attracted by pulleys one of which is driven by a brushed Maxon 370356 DC motor [1]. An other of these maxon motors is mounted on the pendulum but is disconnected and just used as a bearing in this project. Both motors are fitted with an HEDS 5540 optical quadrature encoder allowing for relative position and angle of the cart and pendulum respectively [2].

The motor driving the belt is controlled using a Maxon ADS 50/10 motor controller configured in current control mode. The motor controller takes a $\pm 10\text{ V}$ input signal which then determines the armature current, i_a , see [3].

The primary control unit is a Teensy 3.6 microcontroller board. To program the board through the onboard USB connection a bootloader is used along with the Teensyduino add-on for the Arduino IDE [4].

The encoders are decoded on a shield using Avago HCTL-2021-PLC decoders and read through an 8 bit parallel data bus on the microcontroller board resulting in 2000 tics pr. revolution. This ensures a resolution for the pendulum angle, θ , of $2\pi/2000 = \pi \times 10^{-3}$ rad/tic and $2\pi r/2000 = 2\pi \cdot 0.028/2000 \approx 0.088 \times 10^{-3}$ m/tic for the cart position, x , see [5].

The supply circuit on the microcontroller board is powered by 5V which is regulated to 3.3 V resulting in a 0–3.3 V range for the 12 bit analog output [6]. This output is used to provide the motor controller with an armature current reference, thus, the microcontroller analog output is amplified through the shield to meet the ±10 V input requirement of the motor controller [7].

The following relation between analog 12 bit output values, bit_{DAC} , from the microcontroller and armature current in the motor was found by a previous project group [7],

$$(2.1) \quad \text{bit}_{\text{DAC}} = 105.78 \cdot i_a + 1970 ,$$

and as a result of a force test, see [8], Equation 2.1 was corrected to,

$$(2.2) \quad \text{bit}_{\text{DAC}} = 111.9 \cdot i_a + 1970 ,$$

which is the relation used in this project. All the system parameters used in the design are listed in Table 2.1. It is assumed that all frictions in the system can be modeled as a combination of Coulomb and viscous frictions. Wires hanging from the cart are unmodeled and their weight along with that of the belt are contained in the estimation of the cart mass.

Parameter	Notation	Quantity	Unit
Nominal current (max. continuous current)	I_N	4.58	A
Torque constant	τ_m	93.4×10^{-3}	$\text{N} \cdot \text{m} \cdot \text{A}^{-1}$
Rod Length	l	0.3235	m
Rail Length	l_r	0.89	m
Pulley Radius	r	0.028	m
Pendulum Mass	m	0.201	kg
Cart Mass	M	5.273	kg
Cart Coulomb Friction	$b_{c,c}$	2.884	N
Cart Viscous Friction	$b_{c,v}$	1.680	$\text{N} \cdot \text{m}^{-1} \cdot \text{s}$
Pendulum Coulomb Friction	$b_{p,c}$	0.004	N·m
Pendulum Viscous Friction	$b_{p,v}$	0.4×10^{-3}	$\text{N} \cdot \text{m} \cdot \text{s}$

Table 2.1: The motor parameters, I_N and τ_m , are given by maxon in [1]. The rod length is measured from the pendulum pivot point to the geometrical center of the pendulum. Pendulum mass, rod length, pulley radius and rail length are measured parameters, while cart mass is estimated same as all frictions. The estimations are performed by a previous project group [7].

2.2 Model

The model is based on the generalized coordinates presented in Figure 2.2.

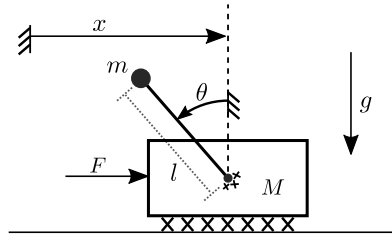


Figure 2.2: Mechanical drawing of the system, where θ is the angle of the pendulum, x is the position of the center of the cart along the rail, F is the applied force and g is the gravitational acceleration. It is indicated that friction is modeled between cart and rail as well as in the pendulum joint.

The pendulum mass center is positioned at zero height at rest s.t. all energies in the system are positive. It is assumed that the pendulum rod is rigid and massless and that the pendulum weights are a point mass at the geometrical center of the weights.

The motor torque is given by direct relation to the armature current by the motor constant, $\tau_m = k_\tau i_a$, such that,

$$(2.3) \quad F = \frac{1}{r} k_\tau i_a \quad [\text{N}]$$

It is well known that the potential energy, U , and the kinetic energy, T , are given by, [9]

$$(2.4) \quad U = mgl(1 + \cos \theta) \quad [\text{J}]$$

$$(2.5) \quad T = \frac{1}{2}(M + m)\dot{x}^2 - ml\cos\theta\dot{\theta} + \frac{1}{2}ml^2\dot{\theta}^2 \quad . \quad [\text{J}]$$

The frictions, indicated in Figure 2.2, are, as mentioned, comprised of Coulomb and viscous frictions with values stated in Table 2.1. The viscous frictions are modeled as linear functions of velocities, [10, 11]

$$(2.6) \quad b_{p,v}\dot{\theta} \quad , \quad b_{c,v}\dot{x} \quad ,$$

for the rotational and linear case respectively. The coulomb frictions are modeled as a constant with its sign depending on the signs of the velocities, such that, [10, 11]

$$(2.7) \quad \operatorname{sgn}(\dot{\theta})b_{p,c} \quad , \quad \operatorname{sgn}(\dot{x})b_{c,c} \quad .$$

This, however, introduces discontinuities at zero velocities. Thus, tanh-functions are used to obtain a continues approximation of the sign-functions,

$$(2.8) \quad \tanh(k_{\tanh}\dot{\theta})b_{p,c} \quad , \quad b_{c,v}\dot{x} - \tanh(k_{\tanh}\dot{x})b_{c,c} \quad ,$$

where $k_{\tanh} = 250$ to increase the steepness of the tanh-functions thereby obtaining a closer approximation of the sign-functions. Finally, by use of the Lagrange-d'Alembert Principle, [9]

$$(2.9) \quad \frac{d}{dt} \frac{\partial \mathcal{L}}{\partial \dot{\mathbf{q}}} - \frac{\partial \mathcal{L}}{\partial \mathbf{q}} = \mathbf{Q} \quad ,$$

where,

$$(2.10) \quad \mathbf{q} = \begin{bmatrix} \theta \\ x \end{bmatrix} \quad , \quad \mathbf{Q} = \begin{bmatrix} -b_{p,v}\dot{\theta} - \tanh(k_{\tanh}\dot{\theta})b_{p,c} \\ \frac{1}{r}k_{\tau}i_a - b_{c,v}\dot{x} - \tanh(k_{\tanh}\dot{x})b_{c,c} \end{bmatrix} \quad ,$$

and $\mathcal{L} = T - U$, the dynamics of the system are found,

$$(2.11) \quad ml^2\ddot{\theta} - ml\cos\theta\ddot{x} - mgl\sin\theta = -b_{p,v}\dot{\theta} - \tanh(k_{\tanh}\dot{\theta})b_{p,c} \quad [\text{N} \cdot \text{m}]$$

$$(2.12) \quad (M + m)\ddot{x} + ml\sin\theta\dot{\theta}^2 - ml\cos\theta\ddot{\theta} = \frac{1}{r}k_{\tau}i_a - b_{c,v}\dot{x} - \tanh(k_{\tanh}\dot{x})b_{c,c} \quad . \quad [\text{N}]$$

By setting up the dynamic equations, Equation 2.12 and 2.11, in the following manner,

$$(2.13) \quad \begin{aligned} & \begin{bmatrix} ml^2 & -ml\cos\theta \\ -ml\cos\theta & M + m \end{bmatrix} \begin{bmatrix} \ddot{\theta} \\ \ddot{x} \end{bmatrix} + \begin{bmatrix} 0 \\ ml\sin\theta\dot{\theta}^2 \end{bmatrix} + \\ & + \begin{bmatrix} -b_{p,v}\dot{\theta} - \tanh(k_{\tanh}\dot{\theta})b_{p,c} \\ \frac{1}{r}k_{\tau}i_a - b_{c,v}\dot{x} - \tanh(k_{\tanh}\dot{x})b_{c,c} \end{bmatrix} + \begin{bmatrix} -mgl\sin\theta \\ 0 \end{bmatrix} = \begin{bmatrix} 0 \\ F \end{bmatrix} \quad , \end{aligned}$$

Chapter 2. System and Model

the general form of an m-link robot is obtained, [12, 13]

$$(2.14) \quad \mathbf{M}(\mathbf{q})\ddot{\mathbf{q}} + \mathbf{C}(\mathbf{q}, \dot{\mathbf{q}}) + \mathbf{B}(\dot{\mathbf{q}}) + \mathbf{G}(\mathbf{q}) = \mathbf{F} \quad ,$$

where,

$\mathbf{M}(\mathbf{q})\ddot{\mathbf{q}}$ is the inertia matrix

$\mathbf{C}(\mathbf{q}, \dot{\mathbf{q}})$ is the Coriolis and centrifugal effects

$\mathbf{B}(\dot{\mathbf{q}})$ is the friction

$\mathbf{G}(\mathbf{q})$ is the force due to gravity

\mathbf{F} is the input force

Part II

Twin Pendulum

Bibliography

- [1] *Maxon Motor*. Aug. 15, 2018. URL: <https://www.maxonmotor.com/maxon/view/product/motor/dcmotor/re/re50/370356>.
- [2] Avago Technologies. *HEDM-55xx/560x & HEDS-55xx/56xx*. Aug. 15, 2018. URL: https://www.infineon.com/dgdl/Infineon-Encoder_HEDS-5540-A14-AP-v01_00-EN.pdf?fileId=5546d46147a9c2e40147d3d593970357.
- [3] *Maxon Controller*. Aug. 15, 2018. URL: <https://www.maxonmotor.com/maxon/view/product/control/Servoerstaerker-4-Q-DC/201583>.
- [4] *sparkfun Teensy 3.6*. Aug. 15, 2018. URL: <https://www.sparkfun.com/products/14057>.
- [5] *HCTL-2021 PLC Avago Datasheet*. Aug. 15, 2018. URL: <https://datasheet.octopart.com/HCTL-2021-PLC-Avago-datasheet-7580518.pdf>.
- [6] *K66 Sub-Family Reference Manual*. Aug. 15, 2018. URL: <https://cdn.sparkfun.com/datasheets/Dev/Arduino/Boards/K66P144M180SF5RMV2.pdf>.
- [7] Jonas Ørndrup Jesper H. Hørgensen. *Non-linear Control and Machine Learning on an Inverted Pendulum on a Cart*. Master Thesis. 2018.
- [8] Niels Skov Vestergaard. *Sliding Mode Stabilization and Phase Plane Trajectory Planning for a Cart Pendulum System*. 9th Semester Project. 2018.
- [9] Rafael Wisniewski. *Mechanical Systems II. Lagrange Mechanics*. Aalborg University, 2013.
- [10] Charles M. Close, Dean K. Frederick, and Jonathan C. Newell. *Modeling and Analysis of Dynamic Systems*. Wiley, 2001.
- [11] H. Olsson et al. *Friction Models and Friction Compensation*. Nov. 28, 1997.
- [12] Mark W. Spong, Seth Hutchinson, and M. Vidyasagar. *Robot Dynamics and Control*. 2nd ed. Wiley, 2005.
- [13] Lorenzo Sciavicco and Bruno Siciliano. *Modelling and Control of Robot Manipulators*. 2nd ed. Lorenzo Sciavicco and Bruno Siciliano. London: Springer, 2012.